Royal Norwegian Council
for Scientific and Industrial Research
(NTNF)

NORSAR

NORSAR Scientific Report No. 1-87/88

Semiannual Technical Summary

1 April — 30 September 1987

L.B. Loughran (ed.)

Kjeller, December 1987

VII.5 Magnitudes of Large Semipalatinsk Explosions using P Coda and Lg Measurements at NORSAR

The objective of this study is to investigate the potential of using NORSAR recorded P coda and Lg waves to obtain stable magnitude estimates of large underground explosions, thereby improving the possibility of obtaining reliable yield estimates from teleseismic recordings.

The NORSAR array (Bungum et al, 1971) has been in operation since 1970. Originally comprising 22 subarrays, with a total of 132 short period vertical seismometers, the array was reduced to 7 subarrays (42 SPZ seismometers) in 1976. In order to obtain consistency over time, this analysis has been restricted to data from these 7 subarrays. With the exception of occasional subarray or instrument outages, this provides for a stable, high quality recording system, making possible reliable comparison of seismic events recorded during the entire time period.

The general characteristics of NORSAR recorded P coda and Lg waves for Semipalatinsk explosions have earlier been studied by Ringdal (1983) and Baumgardt (1985). Ringdal (1983) found by comparing with ISC reported m_b that the use of Lg based magnitudes effectively eliminated the systematic P-wave magnitude differences observed at NORSAR for explosions from the two main test sites within the Semipalatinsk area (Shagan River and Degelen Mountains). Gupta et al (1985) studied NORSAR P and P coda recordings from NTS explosions, and found that P coda measurements provided significantly more precise yields than those based on the initial P. They also obtained promising results in applying P coda measurements to NORSAR recordings from Semipalatinsk explosions.

The propagation path from Semipalatinsk to NORSAR is indicated in Fig. VII.5.1, where also a map of the NORSAR array is shown. In spite of the large epicentral distance (4200 km), the Lg phase can be identified for most explosions of $m_b > 5.0$. However, as shown in the example of Fig. VII.5.2, the Lg amplitude is usually only slightly higher than that of the preceding P coda, and this feature is largely independent of event size.

The data base for this study consists of 72 presumed explosions from the Shagan River area, USSR, covering the time period 1972 to 1987. All such events of ISC $m_b > 5.0$ were included, except for a few cases of NORSAR system outages. The event set is listed in Table VII.5.1, together with ISC or PDE magnitude estimates (m_b) as well as parameters estimated in this study. For most of the events, very accurate location estimates have been computed by Marshall et al (1985), and additional such data have been provided by P. Marshall (personal communication). Otherwise, NEIS or NORSAR location estimates are used. In addition, this study has also made use of maximum likelihood m_b magnitudes estimated at Blacknest from ISC data (P. Marshall, personal communication) and m_b (Lg) estimates published by Nuttli (1986).

Parameter estimation methods

Lg and P coda magnitudes were estimated from NORSAR data for each event using three different methods (for illustration, see Fig. VII.5.2). All three methods were applied to filtered NORSAR SP channels, using a 0.6-3.0 Hz Butterworth bandpass filter. In earlier studies (Rihgdal, 1983), this frequency band has been found to retain the main P and Lg energy while suppressing microseismic noise.

The first method pertains to the Lg phase and comprises direct measurement on individual traces of the largest cycle with a period close to 1 Hz, within a group velocity window of 3.25-3.70 km/s. (The

average Lg group velocity is close to 3.5 km/s.) The amplitude (zero to peak) and the corresponding period were measured and converted to ground motion A_{ij} (i'th event, j'th channel). The amplitudes were then corrected for dispersion, geometrical spreading and anelastic attenuation as described by Nuttli (1986), using parameter values ($Q_0 = 700$, $\xi = 0.4$) derived by Nuttli for the nearby station KON. This resulted in an Lg magnitude estimate MLA_{ij} for each analyzed trace.

Repeating this process for all center instruments of the 7 operational NORSAR subarrays (deleting faulty channels) the NORSAR Lg magnitude MLA was then estimated as:

$$MLA_i = \frac{1}{N} \cdot \sum_{j=1}^{N} MLA_{ij} \qquad (1)$$

where N ($N \leq 7$) is the number of channels.

The second and third methods both comprise automatic RMS measurements of individual channels and pertain to P coda and Lg magnitudes, respectively. For the P coda measurement, a time window of 30 seconds is selected, starting 20 seconds after P onset. The LG window is 2 minutes long, covering the group velocity interval of 3.67 to 3.33 km/s. In addition, a 30 second noise window immediately before P onset was selected for each processed channel. The estimation procedure described in the following was applied for each event to all 42 currently operational NORSAR SP channels, except that faulty channels were deleted.

We denote by s_{ijk} the k'th sample of the filtered trace of event i, instrument j. We define the log mean square L_{ij} by

$$L_{ij} = \log \left[\frac{1}{K} \cdot \sum_{k=1}^{K} s^2_{ijk} \right] \qquad (2)$$

where K is the number of samples in the selected time window. The quantity L_i is defined as

$$L_i = \frac{1}{M} \cdot \sum_{j=1}^{M} L_{ij} \qquad (3)$$

where M($\leq$42) is the number of operative channels.

We denote L_i^N, L_i^C and L_i^L the values of L_i when computed over the noise window (30 seconds, K = 600), P coda window (30 seconds, K = 600) and Lg window (120 seconds, K = 2400), respectively.

The NORSAR P coda RMS magnitudes (MCR_i) and Lg RMS magnitudes (MLR_i) are then estimated by correcting for noise and adjusting to standard scales as follows:

$$MCR_i = 0.5 \cdot \log\left[\exp(L_i^C) - \exp(L_i^N)\right] + B_C \qquad (4)$$

$$MLR_i = 0.5 \cdot \log\left[\exp(L_i^L) - \exp(L_i^N)\right] + B_L \qquad (5)$$

The constants B_C and B_L are determined by the constraints:

$$\sum(MCR_i - MBMLE_i) = 0 \quad (6)$$

$$\sum(MLR_i - MBLG_i) = 0 \quad (7)$$

where $MBLG_i$ is the Lg magnitude given by Nuttli (1986) of the i'th event, $MBMLE_i$ is the maximum likelihood m_b estimate discussed earlier and the sums are taken over all common events.

We also computed uncorrected P coda and Lg magnitudes for purpose of comparison. These were obtained by deleting the noise term in (4) and (5).

Data analysis

The three estimation methods described above were applied to the events in the data set of Table VII.5.1. The procedure to compensate for background noise level had negligible effect on the RMS P coda magnitudes, since the SNR in these cases was consistently high. However, for some of the smaller events (m_b(ISC) $\leq$ 5.6), the effect on RMS Lg was significant, and the resulting estimates must be considered more uncertain than for the large explosions. This is illustrated in Figs. VII.5.3 and VII.5.4, which show, respectively, the uncorrected and corrected RMS Lg estimates plotted against the NORSAR amplitude based Lg magnitudes.

Table VII.5.2 gives a list of standard deviation of magnitude differences for all combinations of sources. We note that the NORSAR P coda magnitude correlate well with ISC maximum likelihood m_b (σ = 0.06), as is also seen from the plot in Fig. VII.5.5. In fact, the

correlation is about as good as between the two ISC-based measurements.

It has earlier been noted by many authors that P coda provides much more stable m_b estimates than the initial P phase, which is subject to strong focussing or defocussing along its ray path. Such effects are to a large extent averaged out in the P coda by various scattering mechanisms. Nevertheless, our analysis has shown that P coda amplitudes across NORSAR are positively correlated with initial P amplitude patterns. Thus, not all of the P focussing/defocussing effects are eliminated, and, by reciprocity, focussing at the source would be expected to significantly affect P coda magnitudes, especially over a larger epicentral area than considered in this paper.

From Table VII.5.2 we also note that the various Lg based measures show surprisingly little correlation with each other, although the RMS noise correction explains much of the scatter between the two Lg estimates based on NORSAR data. Fig. VII.5.6 shows NORSAR RMS Lg versus Nuttli (1986) m_b (Lg) for common events. Even at high magnitudes, where NORSAR noise corrections are insignificant, there is a large scatter. The reasons for this lack of consistency need to be further investigated, but it must be noted that the NORSAR measurements have the advantage of being based on a system stable over time, and with high quality digital recording.

Comparing the Lg based measurements to the ISC maximum likelihood m_b, it appears that the NORSAR RMS Lg shows best correlation (σ = 0.092). Fig. VII.5.7 compares these two magnitude measures, whereas Fig. VII.5.8 shows NORSAR P coda versus NORSAR RMS Lg magnitudes. Comparing these two figures, it is evident that Fig. VII.5.8 has a slightly larger scatter (σ = 0.101) and, moreover, apparently could be split into two subpopulations with parallel trends.

Figs. VII.5.9 and VII.5.10 show that this is no coincidence. On Fig. VII.5.9, the NORSAR P coda - RMS Lg magnitude differences are plotted as a function of event location (Marshall et al (1985) and NEIS data). The P coda - Lg statistics are clearly region dependent within the Shagan River area; in particular the northeast part show consistently low P coda magnitudes, whereas the southwest part shows P coda magnitudes consistently higher than those based on Lg. Fig. VII.5.10 shows that the same trend is apparent when comparing ISC maximum likelihood m_b to NORSAR RMS Lg magnitudes. It is clear that application of regional corrections would improve the mutual consistency of these magnitudes.

Marshall et al (1985) found that explosions in the northeast and southwest portions of the Shagan River area produce distinctly different P waveforms when recorded at the UK seismological array stations, suggesting that the Shagan River site can be subdivided into two test areas characterized by different geophysical properties. Our results support this suggestion. Our data show an average bias $m_b(P) - m_b(Lg)$ of -0.059 ± 0.014 for NE Shagan, and 0.112 ± 0.009 for SW Shagan. Thus, if we attempt to explain this anomaly as resulting from the systematic differences in P recordings only, we obtain a relative $m_b(P)$ bias of about 0.17 m_b units between the two areas. On the other hand, the possibility of an $m_b(Lg)$ bias cannot be ruled out either.

Fig. VII.5.11 illustrates the relative occurrence of large Semipalatinsk explosions after 1976 as a function of NORSAR RMS Lg magnitudes. The plot, which has a nominal vertical scaling, has been obtained by adding Gaussian density functions with standard deviations of 0.015 magnitude units centered at each observed magnitude value. The three clear peaks on this plot might indicate different yield categories. It is interesting to note that the highest magnitude group includes explosions from both the southwest and the northeast areas of Shagan River, whereas similar plots based on P-wave magnitudes would place all of the largest events in the southwest area. The rightmost peak of

the diagram (magnitude 6.06) would correspond to a yield between 150 and 200 kilotons TNT if Nuttli's (1986) formulae are used. With the inherent uncertainty in the absolute calibration level, this is clearly not inconsistent with the 150 kiloton upper limit of the Threshold Test Ban Treaty.

In conclusion, NORSAR based P coda and Lg magnitudes appear to provide magnitude estimates of large Semipalatinsk explosions comparable in stability to those of a world-wide network. There are indications that the Lg based measurements avoid some of the bias inherent in P-based magnitudes. It would furthermore be reasonable to expect that such measurements based on network averaging would provide even better stability. In conjunction with calibration data to obtain accurate absolute reference to yield, such data would appear to provide for very reliable monitoring of a threshold treaty.

F. Ringdal
B.K. Hokland

References

Baumgardt, D.R. (1985): Comparative analysis of teleseismic P coda and Lg waves from underground explosions in Eurasia. Bull. Seism. Soc. Am. 75, 1413-1433.

Gupta, I.N., R.R. Blandford, R.A. Wagner, J.A. Burnetti and T.W. McElfresh (1985): Use of P coda for determination of yield of nuclear explosions. Geophys. J.R. astr. Soc., 83, 2, 541-554.

Marshall, P.D., T.C. Bache and R.C. Lilwall (1985): Body wave magnitudes and locations of Soviet underground explosions at the Semipalatinsk Test Site. AWRE Report No. O 16/84, AWRE, MOD(PE), Aldermaston, Berksh., UK.

Nuttli, O.W. (1986): Lg magnitudes of selected East Kazakhstan underground explosions. Bull. Seism. Soc. Am. 76, 1241-1251.

Ringdal, F. (1983): Magnitudes from P coda and Lg using NORSAR data, in NORSAR Semiannual Technical Summary 1 Oct 82 - 31 Mar 83, NORSAR Sci. Rep. No. 2-82/83, NTNF/NORSAR, Kjeller, Norway.

ORIGIN DATE	ORIGIN TIME	MB	*** LG(AMP)*** MLA	N	STD	*** LG(RMS)*** MLR	N	STD	*** PCODA **** MCR	N	STD
11/02/72	01.26.57.7	6.1	6.132	7	0.040	6.121	42	0.069	6.207	42	0.058
12/10/72	04.27.07.7	6.0	6.157	7	0.066	6.120	42	0.068	6.013	42	0.079
07/23/73	01.22.57.8	6.1	6.185	7	0.082	6.199	41	0.078	6.286	41	0.060
12/14/73	07.46.57.0	5.8	5.951	7	0.087	5.876	42	0.063	5.826	39	0.074
10/16/74	06.32.57.5	5.5	5.455	7	0.086	5.413	42	0.062	5.596	42	0.065
12/27/74	05.46.56.8	5.6	5.849	7	0.054	5.711	42	0.060	5.512	42	0.093
04/27/75	05.36.57.3	5.6	5.677	7	0.060	5.550	42	0.054	5.732	42	0.072
10/29/75	04.46.57.5	5.8	5.755	7	0.100	5.632	42	0.062	5.733	42	0.057
12/25/75	05.16.57.0	5.7	5.817	7	0.053	5.804	42	0.067	0.000	0	0.000
04/21/76	05.02.57.4	5.3	0.000	0	0.000	0.000	0	0.000	5.226	42	0.062
06/09/76	03.02.57.6	5.3	5.462	7	0.091	5.203	42	0.056	5.126	42	0.093
07/04/76	02.56.57.7	5.8	5.831	7	0.036	5.813	42	0.063	5.909	42	0.075
08/28/76	02.56.57.5	5.8	5.762	7	0.085	5.737	41	0.069	5.761	41	0.063
05/29/77	02.56.57.8	5.8	5.788	7	0.066	5.669	39	0.061	5.796	41	0.057
06/29/77	03.06.58.0	5.3	5.274	7	0.021	5.070	39	0.054	5.279	40	0.072
09/05/77	03.02.57.8	5.8	5.953	7	0.075	5.891	39	0.067	5.789	40	0.072
10/29/77	03.07.02.9	5.6	5.889	7	0.083	5.784	39	0.061	5.768	41	0.070
06/11/78	02.56.57.7	5.9	5.824	7	0.066	5.752	39	0.059	5.918	39	0.072
07/05/78	02.46.57.3	5.8	5.823	7	0.086	5.789	39	0.057	5.877	39	0.066
08/29/78	02.37.06.5	5.9	6.005	7	0.060	6.006	39	0.057	5.914	39	0.090
09/15/78	02.36.57.3	6.0	5.948	7	0.093	5.906	38	0.059	5.979	41	0.077
11/04/78	05.05.57.5	5.6	5.906	7	0.039	5.691	39	0.061	5.631	41	0.069
11/29/78	04.33.02.9	6.0	5.982	7	0.086	5.969	39	0.067	6.004	41	0.070
06/23/79	02.56.57.6	6.2	6.088	4	0.084	6.065	21	0.070	6.174	23	0.057
07/07/79	03.46.57.4	5.8	5.996	7	0.091	5.967	39	0.074	5.850	41	0.071
08/04/79	03.56.57.2	6.1	6.105	7	0.032	6.098	39	0.062	6.170	41	0.076
10/28/79	03.16.56.9	6.0	6.060	6	0.056	6.033	39	0.063	5.936	41	0.085
12/02/79	04.36.57.5	6.0	5.962	5	0.046	5.903	33	0.067	6.074	35	0.050
06/29/80	02.32.57.7	5.7	5.722	4	0.073	5.676	28	0.094	5.794	25	0.049
09/14/80	02.42.39.3	6.2	0.000	0	0.000	0.000	0	0.000	6.222	36	0.049
10/12/80	03.34.14.1	5.9	5.946	6	0.043	5.912	39	0.061	5.840	41	0.089
12/14/80	03.47.06.6	5.9	5.887	5	0.075	5.911	39	0.045	5.965	41	0.070
12/27/80	04.09.08.2	5.9	5.948	5	0.040	5.908	39	0.076	5.949	41	0.069
03/29/81	04.03.50.0	5.6	5.719	5	0.052	5.521	39	0.053	5.519	41	0.070
04/22/81	01.17.11.4	6.0	5.945	5	0.060	5.888	33	0.046	5.991	35	0.065
05/27/81	03.58.12.1	5.5	5.576	4	0.020	5.442	27	0.061	5.320	29	0.098
09/13/81	02.17.18.2	6.1	6.115	6	0.081	6.092	34	0.076	6.129	35	0.071
10/18/81	03.57.02.6	6.1	5.951	7	0.072	5.976	39	0.057	6.069	35	0.065
11/29/81	03.35.08.7	5.7	5.789	5	0.078	5.566	33	0.062	5.693	35	0.071
12/27/81	03.43.14.1	6.2	6.046	6	0.040	6.056	39	0.074	6.183	41	0.065
04/25/82	03.23.05.4	6.1	6.074	6	0.072	6.056	39	0.077	6.111	39	0.071
07/04/82	01.17.14.4	6.1	0.000	0	0.000	0.000	0	0.000	6.078	32	0.089
08/31/82	01.31.00.5	5.3	0.000	0	0.000	0.000	0	0.000	5.356	39	0.065
12/05/82	03.37.12.6	6.1	5.989	6	0.088	5.968	37	0.078	6.076	36	0.060
12/26/82	03.35.14.1	5.7	5.834	5	0.065	5.653	39	0.061	5.731	29	0.061
06/12/83	02.36.43.5	6.1	6.051	5	0.077	6.070	24	0.071	6.132	24	0.072
10/06/83	01.47.06.5	6.0	5.917	4	0.021	5.876	18	0.054	6.034	18	0.068
10/26/83	01.55.04.8	6.1	5.996	6	0.076	5.993	32	0.055	6.097	32	0.065
11/20/83	03.27.04.4	5.5	0.000	0	0.000	0.000	0	0.000	5.481	32	0.071

Table VII.5.1 List of events used in this study. The table includes date, origin time, m_b(ISC/PDE) as well as NORSAR based measurements discussed in the text and standard deviations across NORSAR. Zero entries indicate either no NORSAR data available or SNR too low for reliable measurement.

ORIGIN DATE	ORIGIN TIME	MB	*** LG(AMP)*** MLA	N	STD	*** LG(RMS)*** MLR	N	STD	*** PCODA **** MCR	N	STD
02/19/84	03.57.03.4	5.9	5.764	5	0.053	5.724	27	0.051	5.889	27	0.057
03/07/84	02.39.06.4	5.7	5.775	5	0.075	5.696	27	0.058	5.632	27	0.073
03/29/84	05.19.08.2	5.9	5.905	5	0.035	5.897	27	0.057	5.889	27	0.071
04/25/84	01.09.03.5	6.0	5.905	6	0.072	5.862	33	0.066	5.972	33	0.071
05/26/84	03.13.12.4	6.0	6.075	6	0.063	6.064	33	0.064	5.965	33	0.115
07/14/84	01.09.10.5	6.2	6.089	6	0.073	6.043	33	0.074	6.148	31	0.088
10/27/84	01.50.10.6	6.2	6.101	6	0.077	6.075	32	0.067	6.254	32	0.073
12/02/84	03.19.06.3	5.8	5.973	5	0.141	5.864	27	0.076	5.747	25	0.081
12/16/84	03.55.02.7	6.1	6.055	5	0.093	6.030	27	0.066	6.113	27	0.068
12/28/84	03.50.10.7	6.0	6.009	6	0.057	5.978	33	0.073	6.147	33	0.073
02/10/85	03.27.07.6	5.9	5.898	7	0.070	5.791	38	0.069	5.947	39	0.068
04/25/85	00.57.06.5	5.9	5.979	5	0.078	5.850	27	0.065	5.936	29	0.069
06/15/85	00.57.00.7	6.0	6.024	5	0.075	5.966	28	0.062	6.099	28	0.069
06/30/85	02.39.02.7	6.0	5.983	4	0.068	5.917	28	0.059	6.058	28	0.065
07/20/85	00.53.14.5	5.9	5.884	7	0.076	5.855	36	0.071	5.912	36	0.068
03/12/87	01.57.17.0	5.4	5.385	6	0.081	5.223	31	0.059	5.437	33	0.068
04/03/87	01.17.08.0	6.2	6.062	6	0.079	6.048	31	0.070	6.245	32	0.052
04/17/87	01.03.04.0	6.0	5.928	6	0.072	5.895	31	0.069	6.077	32	0.060
06/20/87	00.53.04.0	6.1	5.992	7	0.117	5.962	34	0.070	6.124	37	0.092
08/02/87	00.58.08.0	5.9	5.945	6	0.103	5.866	30	0.074	5.885	30	0.074
11/15/87	03.31.08.0	6.0	6.024	7	0.088	5.959	34	0.063	6.098	36	0.058
12/13/87	03.21.08.0	6.0	6.094	6	0.088	6.066	29	0.080	6.081	30	0.066
12/27/87	03.05.08.0	6.0	6.109	6	0.106	6.032	30	0.083	6.211	30	0.052
AVERAGE STANDARD DEVIATIONS:					0.070			0.064			0.069
STANDARD DEVIATION OF MEAN VALUES:					0.028			0.011			0.012

Table VII.5.1 (cont.)

	ISC/PDE	ISC(M-L)	MB(LG)	PCODA	LG(RMS)	LG(AMP)
ISC/PDE	0.000	0.066	0.119	0.068	0.093	0.109
ISC(M-L)	0.066	0.000	0.120	0.060	0.092	0.136
MB(LG)	0.119	0.120	0.000	0.127	0.116	0.135
PCODA	0.068	0.060	0.127	0.000	0.101	0.130
LG(RMS)	0.093	0.092	0.116	0.101	0.000	0.065
LG(AMP)	0.109	0.136	0.135	0.130	0.065	0.000

Table VII.5.2 Standard deviations of differences between various magnitude estimates discussed in the text.

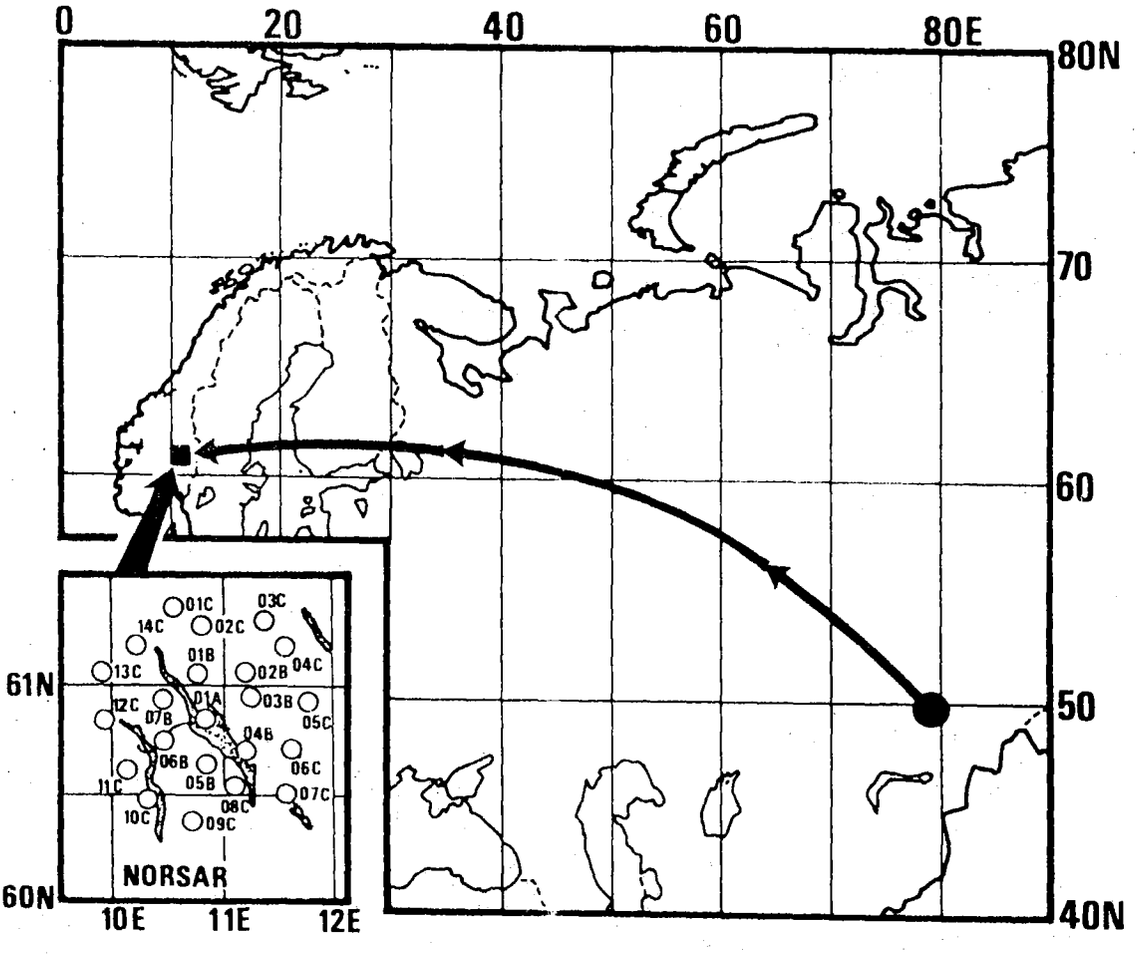

Fig. VII.5.1 Map showing the propagation path from Semipalatinsk to NORSAR (distance approximately 4200 km). The original NORSAR array configuration is also displayed.

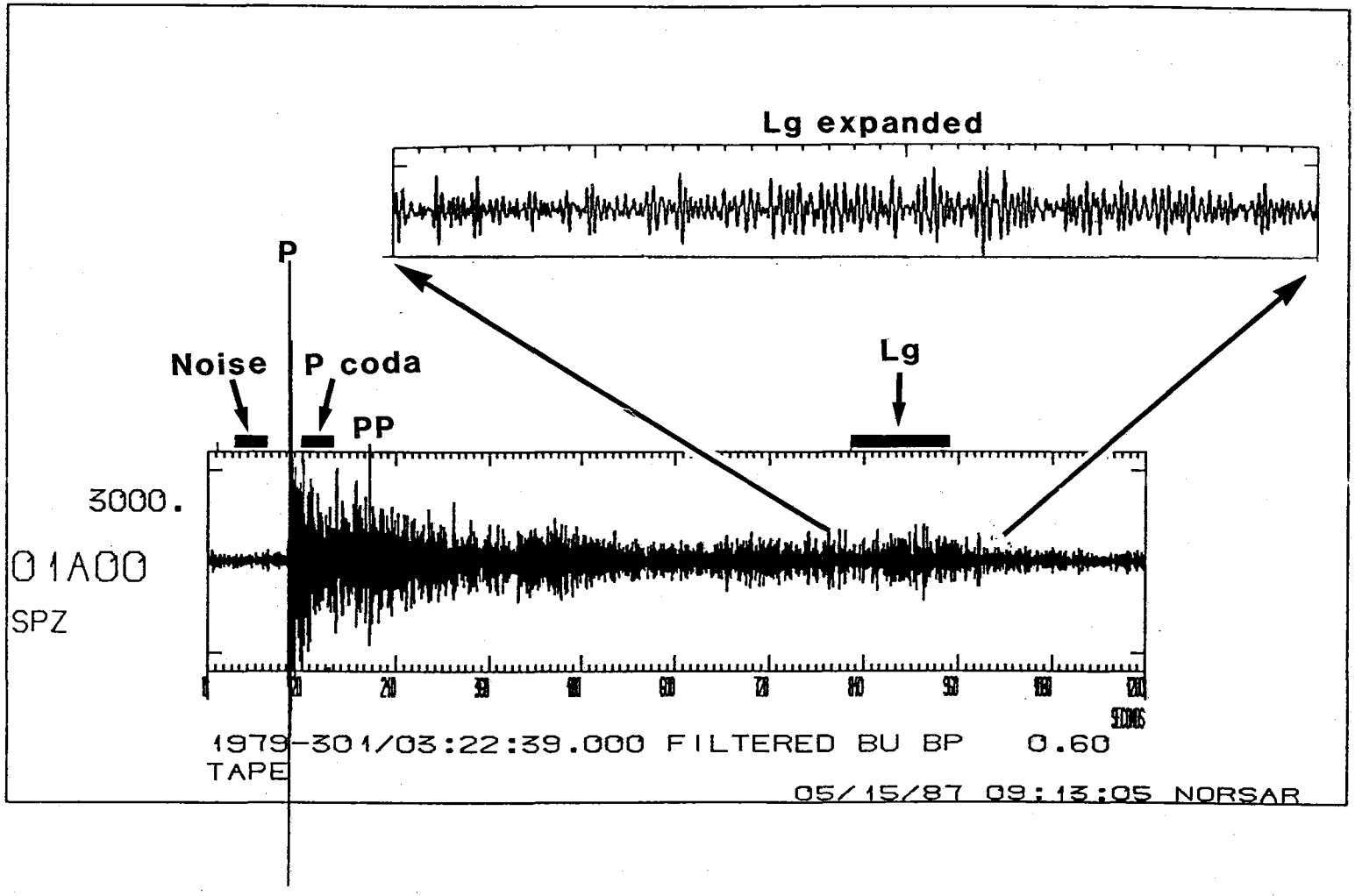

Fig. VII.5.2 Example of a typical NORSAR-recording of a Semipalatinsk explosion (instrument 01A00). The plot covers 20 minutes of data filtered in the passband 0.6-3.0 Hz. The time windows used for RMS Lg, RMS P coda and RMS noise measurements as described in the text are indicated. An expanded plot is shown of the portion of the trace used for NORSAR Lg amplitude.

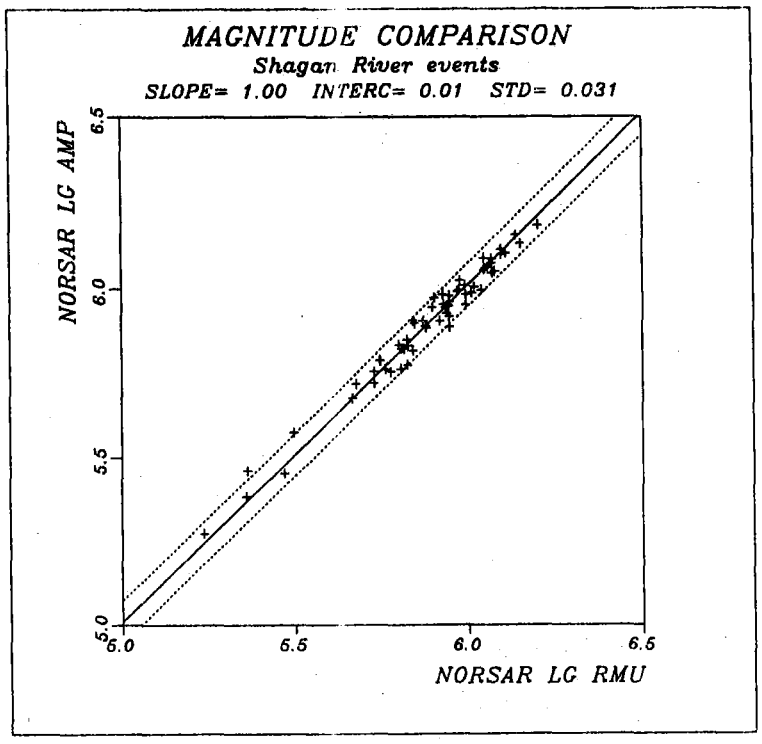

Fig. VII.5.3 Plot of amplitude based NORSAR Lg magnitudes versus NORSAR RMS Lg magnitudes. In this plot no noise correction has been applied. The slope has been restricted to 1.00, and the dotted lines correspond to plus/minus two standard deviations.

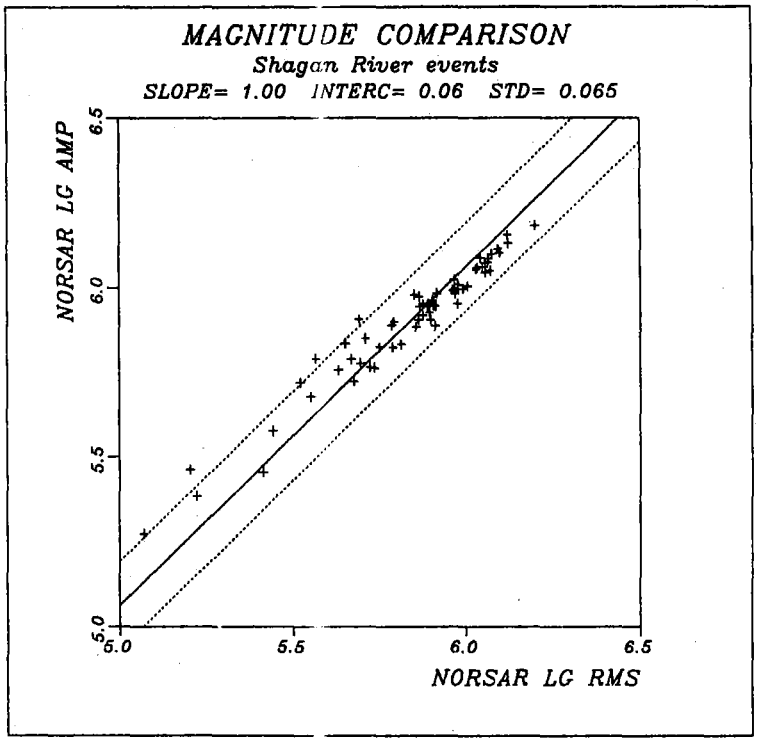

Fig. VII.5.4 Same as Fig. VII.5.3, except that the NORSAR RMS Lg magnitudes have been corrected for noise as discussed in the text. Note the effect of this at low magnitudes.

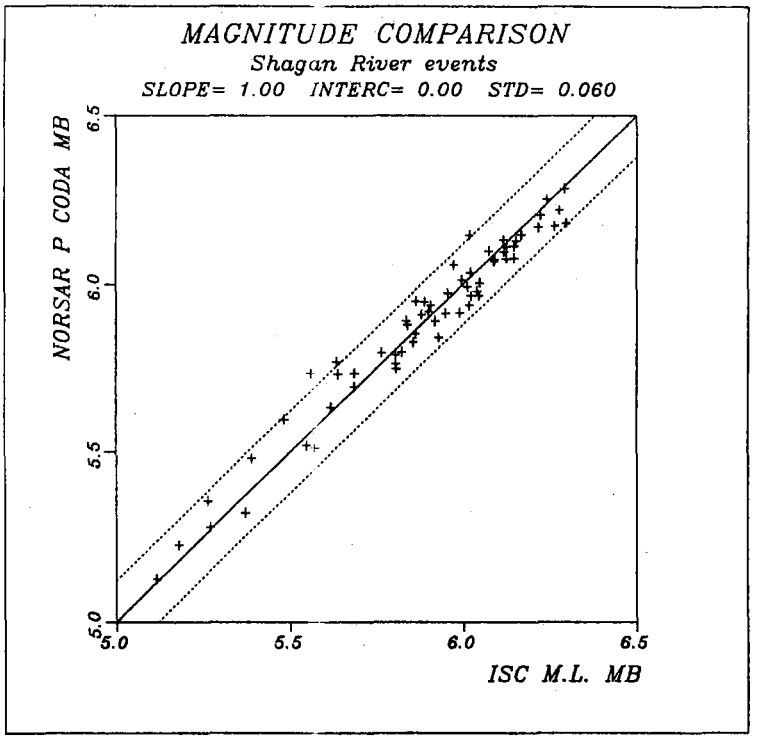

Fig. VII.5.5 Plot of NORSAR P coda magnitudes versus ISC maximum likelihood m_b. (Slope restricted to 1.00; dotted lines correspond to plus/minus two standard deviations.)

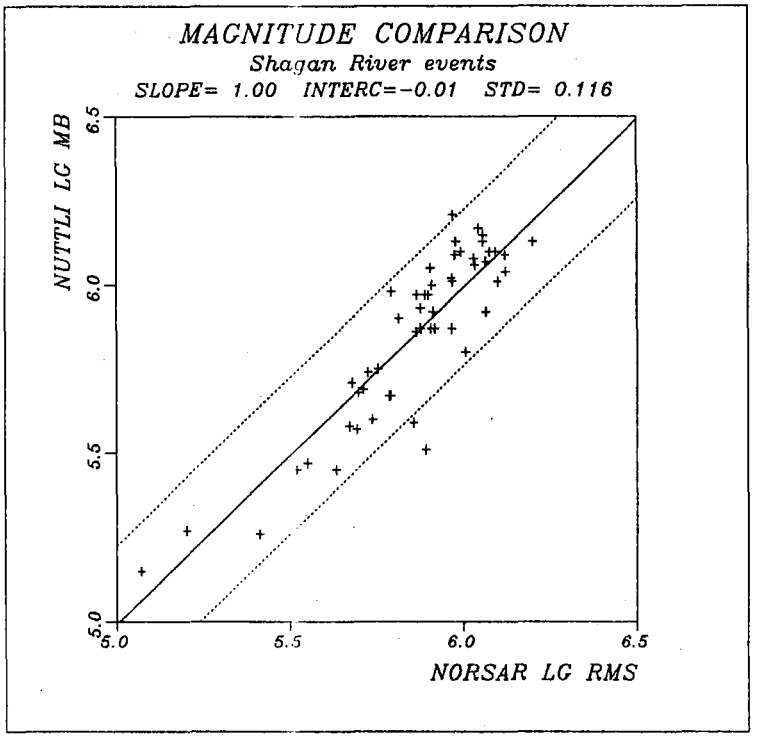

Fig. VII.5.6 Plot of Nuttli (1986) m_b (Lg) versus NORSAR Lg RMS magnitudes. The slope and dotted lines are defined as in Fig. VII.5.5. Note the significant scatter even at high magnitudes.

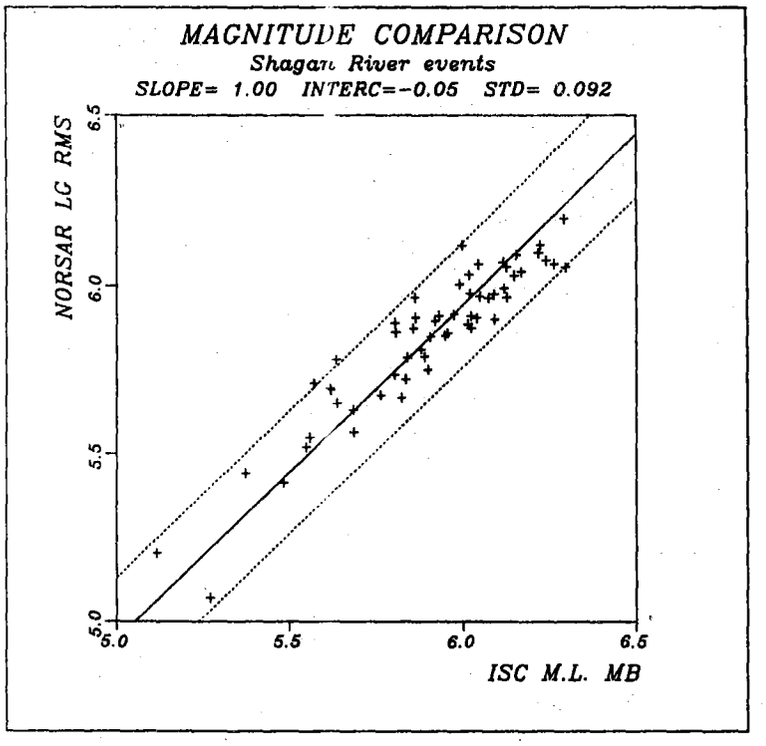

Fig. VII.5.7 Plot of ISC maximum likelihood m_b versus NORSAR Lg RMS magnitudes. The slope and dotted lines are defined as in Fig. VII.5.5.

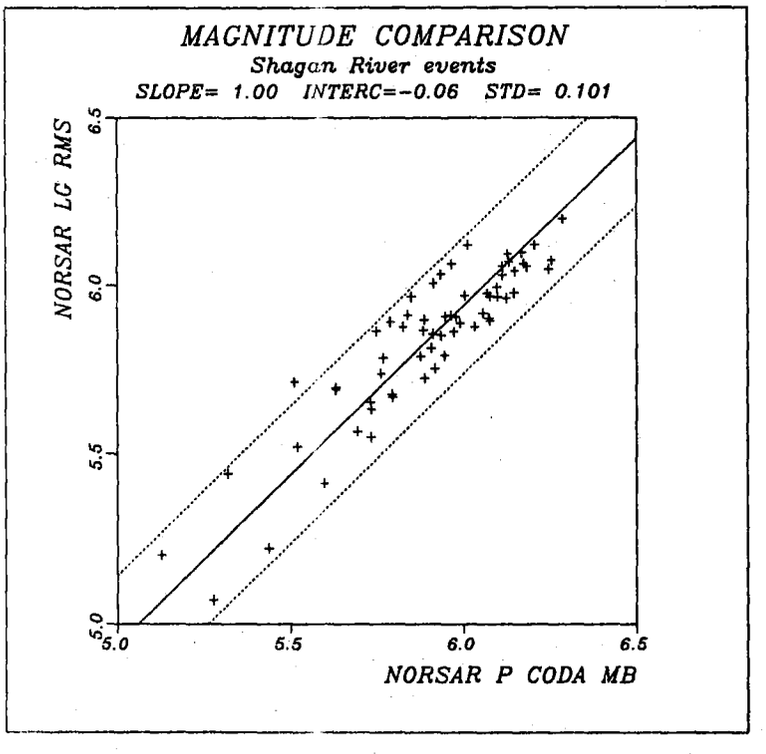

Fig. VII.5.8 Plot of NORSAR RMS P coda m_b versus NORSAR RMS Lg magnitudes. The slope and dotted lines are defined as in Fig. VII.5.5.

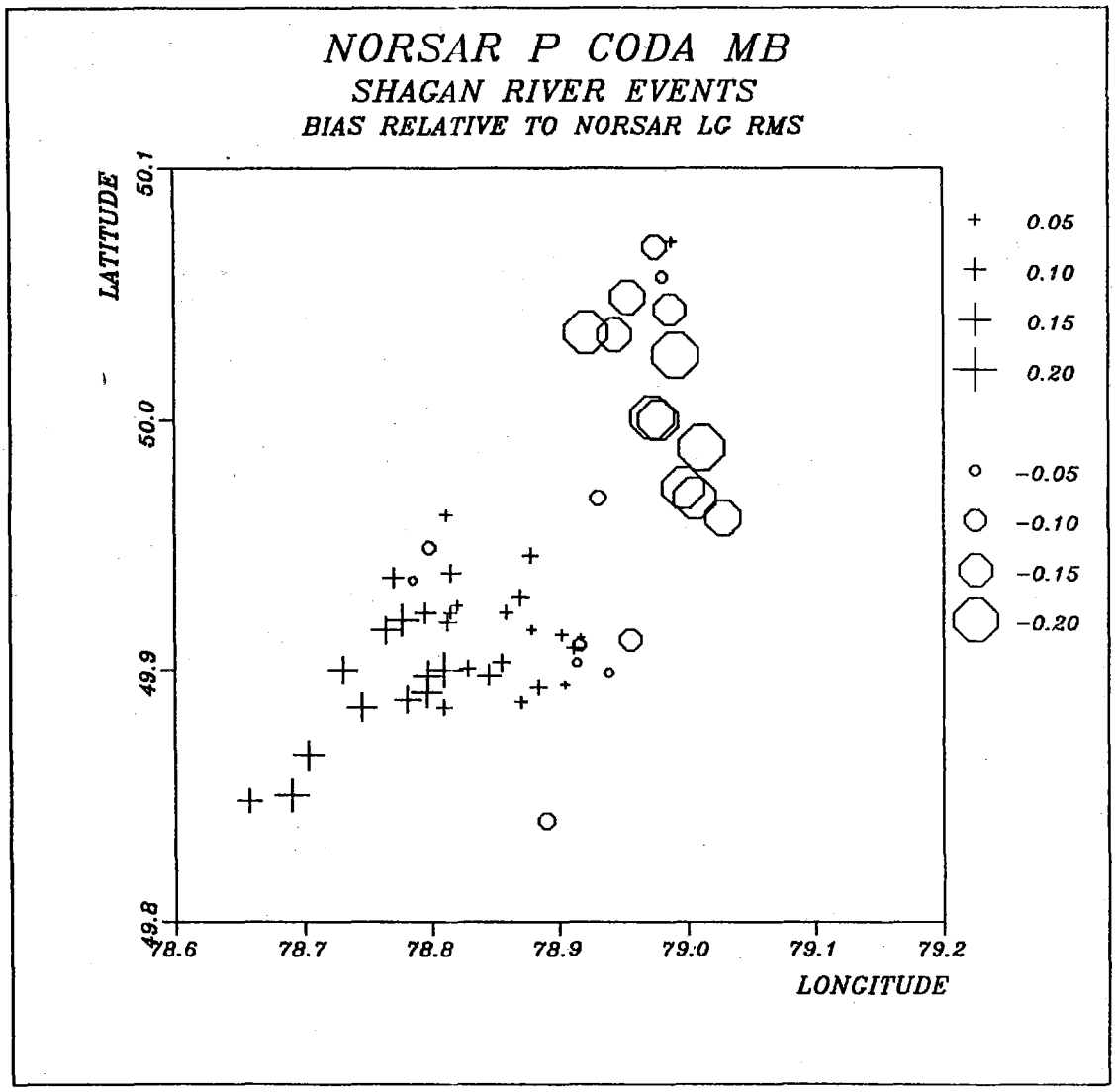

Fig. VII.5.9 Plot of magnitude residuals (NORSAR P coda minus NOkSAR Lg RMS magnitudes) as a function of event location for events of $m_b \geq 5.60$. Plusses and circles correspond to residuals greater or less than the average, respectively, with symbol size proportional to the deviation. Location estimates are those of Marshall et al (1985) where available, otherwise NEIS estimates have been used. Note the systematic variation within the Shagan River area.

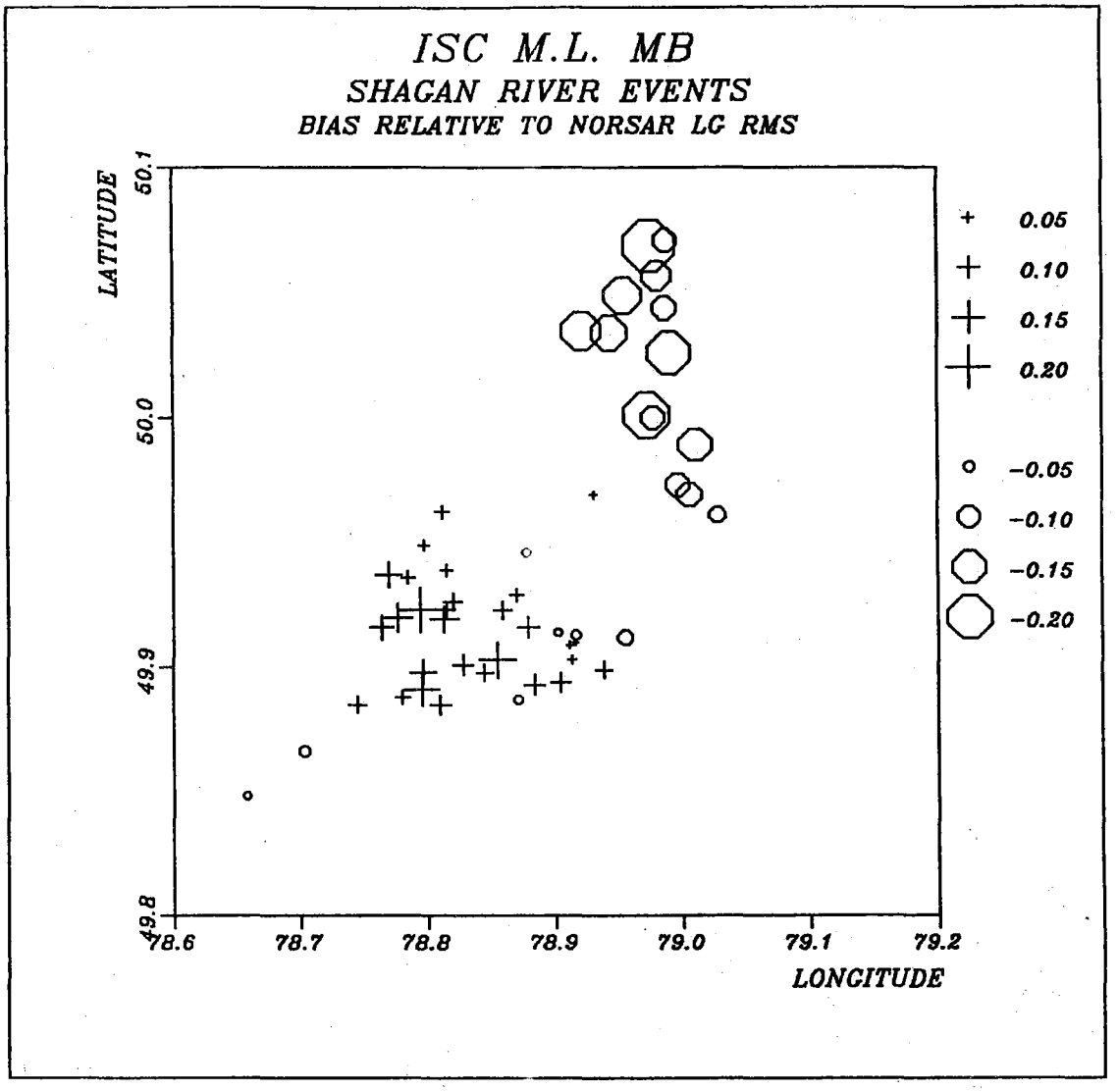

Fig. VII.5.10 Same as Fig. VII.5.9, except that the residual corresponds to ISC maximum likelihood m_b minus NORSAR Lg RMS magnitudes. Note the similarities with Fig. VII.5.9.

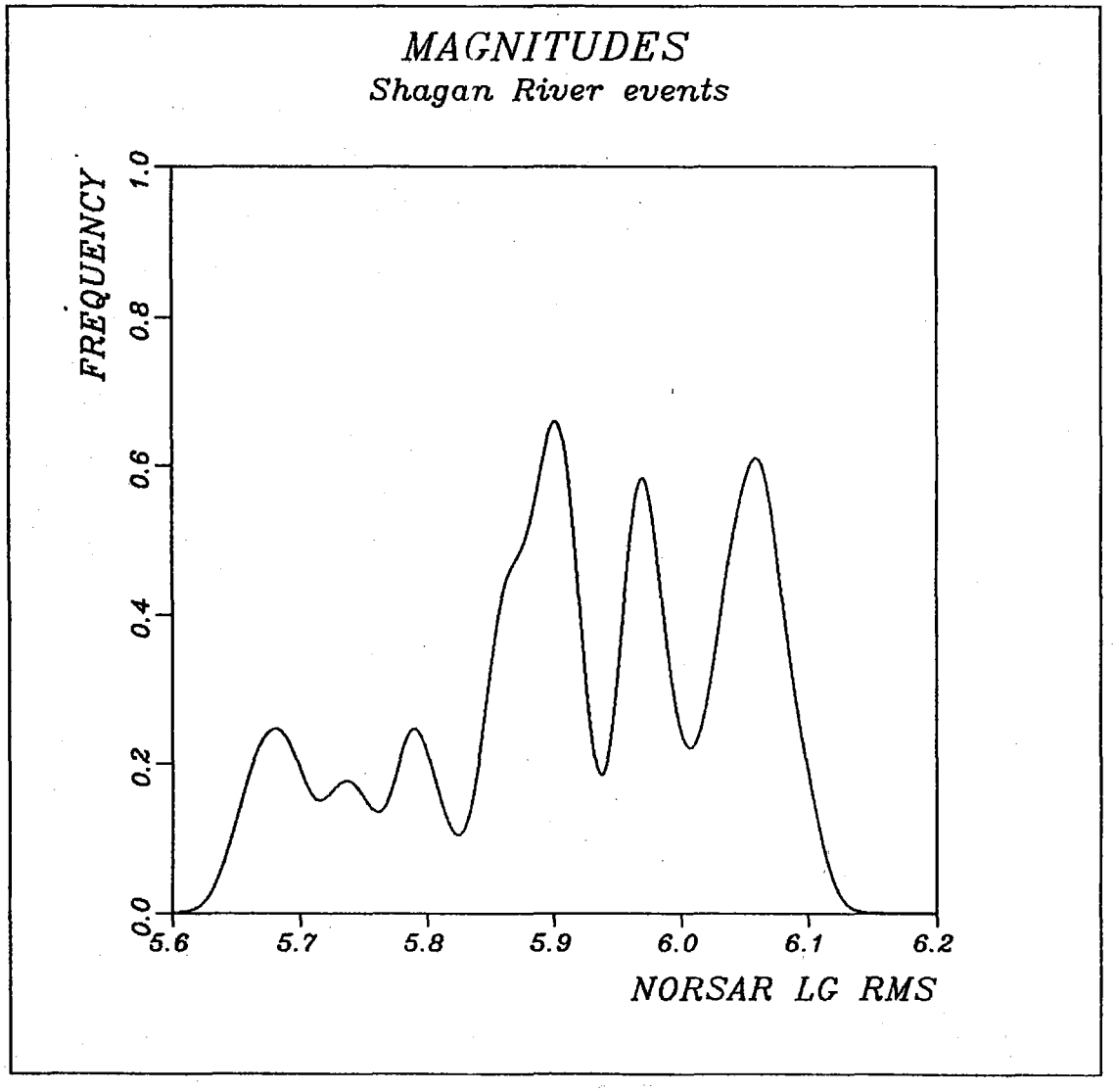

Fig. VII.5.11 Relative frequency of occurrence of large Shagan River explosions after 1976, based on estimated NORSAR Lg RMS magnitudes. The figure has been generated by adding Gaussian probability density functions with standard deviations of 0.015 centered at each magnitude value. Note the three distinct peaks in the diagram.